HHS Public Access

Author manuscript

J Biomater Appl. Author manuscript; available in PMC 2016 October 01.

Published in final edited form as:

J Biomater Appl. 2015 October ; 30(4): 435–449. doi:10.1177/0885328215590967.

Effect of Low Temperature Ethylene Oxide and Electron Beam Sterilization on the In Vitro and In Vivo Function of Reconstituted Extracellular Matrix-Derived Scaffolds

Benedikt L. Proffen, MD[1], **Gabriel S. Perrone, MS**[1], **Braden C. Fleming, PhD**[2], **Jakob T. Sieker, MD**[1], **Joshua Kramer, DVM**[3], **Michael L. Hawes, DVM**[3], and **Martha M. Murray, MD**[1]

Benedikt L. Proffen: Benedikt.proffen@childrens.harvard.edu; Gabriel S. Perrone: Gabriel.perrone@childrens.harvard.edu; Braden C. Fleming: Braden_fleming@brown.edu; Jakob T. Sieker: Jakob.sieker@childrens.harvard.edu; Joshua Kramer: jkramercps@gmail.com; Michael L. Hawes: mhawes.cps@comcast.net; Martha M. Murray: Martha.Murray@childrens.harvard.edu

[1]Department of Orthopaedic Surgery, Sports Medicine Research Laboratory, Children's Hospital Boston/Harvard Medical School, Enders Building, Room 270, 300 Longwood Avenue; Boston, MA 02115, Phone: (617) 919-2540; FAX: (617) 730-0789

[2]Department of Orthopaedics, Bioengineering Labs, Warren Alpert Medical School of Brown University/Rhode Island Hospital, CORO West, Suite 404, 1 Hoppin Street, Providence, RI 02903, Phone: (401) 444-5444; FAX: (401) 444-4418

[3]Charter Preclinical Services, 21 Main St., Suite 3A, Hudson, MA 01749, Phone: (978) 212-5428; FAX: (508) 789-1537

Abstract

Reconstituted extracellular matrix (ECM) -derived scaffolds are commonly utilized in preclinical tissue engineering studies as delivery vehicles for cells and growth factors. Translation into clinical use requires identifying a sterilization method that effectively removes bacteria but doesn’t harm scaffold function.

To determine effectiveness of sterilization and impact on ECM scaffold integrity and function low temperature ethylene oxide and 15kGy electron beam irradiation techniques were evaluated. Scaffold sterility was assessed in accordance to United States Pharmacopeia Chapter 71. Scaffold matrix degradation was determined in vitro using enzymatic resistance tests and gel electrophoresis. Scaffold mechanics including elastic modulus, yield stress and collapse modulus were tested. Lastly, 14 Yorkshire pigs underwent ACL transection and bio-enhanced ACL repair using sterilized scaffolds. Histologic response of ligament, synovium and lymph nodes was compared at 4, 6, and 8 weeks.

Ethylene oxide as well as electron beam irradiation yielded sterile scaffolds. Scaffold resistance to enzymatic digestion and protein integrity slightly decreased after electron beam irradiation while ethylene oxide altered scaffold matrix. Scaffold elastic modulus and yield stress were increased

Corresponding Author: Benedikt L. Proffen, Department of Orthopaedic Surgery, Sports Medicine Research Laboratory, Children's Hospital Boston/Harvard Medical School, Enders Building, Room 270, 300 Longwood Avenue 02115; Phone: (617) 919-2540; FAX: (617) 730-0789; Benedikt.Proffen@childrens.harvard.edu.

AUTHOR DISCLOSURE STATEMENT.

The authors have no conflicts of interest in relation to this material to disclose. No competing financial interests exist.

after electron beam treatment, while collapse modulus was increased after ethylene oxide treatment. No significant changes in ACL dimensions, *in vivo* scaffold resorption rate, or histologic response of synovium, ligament and lymph nodes with either terminal sterilization technique were detectable.

In conclusion, this study identifies two methods to terminally sterilize an ECM scaffold. *In vitro* scaffold properties were slightly changed without significantly influencing the biologic responses of the surrounding tissues *in vivo*. This is a critical step toward translating new tissue engineering strategies to clinical trials.

Keywords

Anterior cruciate ligament; extra-cellular matrix; scaffold; low temperature ethylene oxide; electron beam irradiation

INTRODUCTION

Tissue engineering is a field with immense promise for improving the health care of patients. The endless combinations of scaffolds, cells and growth factors have led to hundreds of publications evaluating these technologies in vitro and in vivo. However, less is known about translating these technologies to clinical use. One major hurdle for scaffolds made from naturally occurring extracellular matrix materials (ECM-derived scaffolds) is terminal sterilization. Terminal sterilization involves sterilizing the product inside a sterile barrier system at the end of the manufacturing process as a final step before delivery to the clinic. Terminal sterilization is the standard for medical devices, even those which have been produced using aseptic technique. The use of terminal sterilization provides assurance that even if contamination is unintentionally introduced at any point during device manufacture, it will be mitigated by the sterilization process. The FDA requires the sterilization process to reliably remove all microbial contamination(1), which, if successful, guarantees a more repeatable process and sterility assurance level (SAL) than aseptic processing alone.(2) The SAL for a medical device is set to 10^{-6}, equivalent to one device in a million with measurable contamination.(3)

Traditional sterilization methods utilizing heat (autoclaving, dry heat) for sterilization of ECM-derived scaffolds are not applicable, since most matrix proteins, specifically collagen, are irreversibly denatured at temperatures over 60–65°C.(4) Therefore, the most frequently used alternative low temperature sterilization methods for temperature sensitive ECM-derived devices are ethylene oxide (ETO) and high-energy radiation (electron beam or gamma radiation).(5) The industrial standards (ISO 11135-1) (6) and (ISO 11137-2) (7) suggest that low temperature ethylene oxide and 15 kGy electron beam irradiation dose will lead to a log reduction of 10^{-6} colony forming units of bacteria and fungi when used on a material with a low initial bioburden (i.e. those manufactured using aseptic technique).(8, 9) Literature concerning the effects of sterilization utilizing the two mentioned methods mostly focuses on decellularized ECM tissue, and insufficiently covers the sterilization of reconstituted ECM-derived scaffolds. In any case, ethylene oxide can change sensitive protein structures of ECM-derived scaffolds by reacting with the free amine groups of the

collagen proteins.(10) Ethylene oxide has also been demonstrated to decrease the mechanical properties of an ECM-derived scaffold designed for bladder reconstruction,(11) and to reduce the metabolic activity of cells in a small intestinal submucosa (SIS) graft after implantation.(12) High-energy radiation as well can alter proteins directly by cleaving the protein chains, or indirectly by causing the buildup of free radicals in the surrounding atmosphere which themselves react with the protein groups and change protein structure. (4, 13, 14) Because some studies have shown a lesser reduction of the in vitro mechanical properties of ECM-derived scaffolds after electron beam sterilization when compared to gamma irradiation, electron beam radiation is generally the preferred irradiation method for ECM-derived devices.(15) Still, when comparing low temperature ethylene oxide with electron beam sterilization, the former seems to have a lesser effect on the *in vitro* mechanical properties and protein structure of dermal sheep collagen.(14). What effects the sterilization has on the *in vitro* properties of reconstituted ECM-derived scaffolds and how changes *in vitro* properties can influence the *in vivo* response to ECM-derived scaffolds hasn't been analyzed, yet.

The first aim was to determine whether a reconstituted ECM-derived scaffold could be terminally sterilized using low temperature ethylene oxide or low dose 15kGy electron beam irradiation. The second aim was to assess whether the sterilization process would result in changes in the protein structure and scaffold mechanics *in vitro*. The third aim was to establish if the sterilization process would change the *in vivo* resorption rate of the scaffold or lead to an altered response of the surrounding tissue. The hypotheses of this study were based on earlier findings in the literature, in which electron beam and low temperature ethylene oxide treatment were compared. The ethylene oxide method had a less of an effect on the *in vitro* mechanical properties and protein structure of dermal sheep collagen.(14) This led to the hypotheses that both the ethylene oxide and electron beam methods would effectively sterilize the ECM scaffold, and that the electron beam sterilization process would decrease protein integrity and change the biomechanical properties and enzymatic resistance of the scaffold *in vitro* as well as healing response *in vivo*, but increase scaffold resorption rate and tissue reaction *in vivo*.

MATERIALS AND METHODS

Preparation of the reconstituted ECM-derived scaffold

A total of 86 ECM-derived scaffolds (MIACH, Boston Children's Hospital, Boston, MA) were manufactured from a single production as previously described.(16) Briefly, bovine connective tissue from the knee capsule was harvested aseptically, decellularized using a detergent solution, pepsin-solubilized and the collagen concentration of the solution adjusted to greater than 10 mg/ml and lyophilized in a vial to yield a dry, porous ECM cylinder 22 mm in diameter and 30 mm in length. For all scaffolds, aseptic processing techniques were used with no observed deviation from sterile technique. Polyethylene/Tyvek pouches were used as a sterile barrier for all scaffolds. Scaffolds were divided according to the study design (Table 1).

Terminal Sterilization

30 scaffolds were terminally sterilized using a validated low temperature (< 40°C) ethylene oxide cycle (scaffolds of the ETO group) in a 3M Steri-Vac Sterilizer (3M, St. Paul, MN) with a gas dwell time of 4.75 hours, relative humidity of 55% and a gas concentration of 650mg/L. For electron beam irradiation, a dose map was created by distributing 6 dosimeters in the plane of the scaffolds inside the radiation field to verify a minimum radiation exposure of the scaffolds of 15 kGy. 30 scaffolds were irradiated at ambient temperature with a single dose of 15 kGy (Synergy Health, Saxonburg, PA, USA) (scaffolds of the EBEAM group). 26 additional scaffolds were packaged using aseptic technique, but not terminally sterilized (scaffolds of the ASEPTIC group). All ASEPTIC, ETO, and EBEAM scaffolds were stored at room temperature and shielded from sunlight until use.

Sterility Testing

8 scaffolds from each lot of ASEPTIC, ETO and EBEAM scaffolds were tested for sterility in accordance to the United States Pharmacopeia Chapter 1032 (USP <1032>) in a certified laboratory (Microtest Laboratories, Inc. Agawam, MA, USA).(17) According to contractor information, scaffolds were incubated in either trypticase soy broth – for detection of common aerobic and facultatively anaerobic bacteria – or fluid thioglycollate medium – a differential medium to determine the oxygen requirements of microorganisms. For each media type, 4 randomly chosen scaffolds from each lot (ASEPTIC, ETO, EBEAM) were incubated in the media at 32.5 ± 2.5 °C for 7 days. Samples were evaluated visually for cloudiness or pellicle formation as an indicator of bacterial and fungal growth. A bacteriostasis/fungostasis test was performed on the scaffolds as well, during which scaffolds were transferred to growth media, inoculated with microorganisms and monitored for growth to assure the absence of antimicrobial properties of the scaffolds and thus validate the sterility results.

In Vitro Assessment of Scaffold

ECM scaffolds were assessed for their macroscopic porous structure, integrity of their protein molecules as well as their resistance to enzymatic digestion. Briefly, to visualize macroscopic porous structure, two discs measuring 10mm in length were cut transversely from three scaffolds each per group. Cut surfaces were recorded using a Keyence VHX 2000 Digital Microscope (Keyence, Itasca, IL, USA). The same discs were used to measure the time to full absorption of 1 ml of whole blood.

To assess protein integrity, 30 mg from three scaffold samples per group (ASEPTIC, ETO and EBEAM) was homogenized in hydrochloric acid solution. Sodium dodecyl sulfate polyacrylamide gel electrophoresis (SDS-PAGE) using reagents and gels from BIO-RAD (BIO-RAD, Hercules, CA) was used to separate out the component proteins. The protein band pattern was visually analyzed on a gel and compared to a standard protein ladder. Resistance to enzymatic digestion for all groups was tested on cylinder punch outs from the same three scaffolds used for the SDS-PAGE. Cylinder punch outs had a diameter of 8mm and thickness of 7mm. 6 punch outs from each group were placed in culture with one of three enzymes: collagenase (250ug/ml in phosphate buffered saline (PBS)), elastase (100ug/ml in PBS), or plasmin digestion solution (40ug/ml in water). These concentrations

were chosen based on prior reports of the concentration of these enzymes in post-traumatic synovial fluid.(18, 19) All groups were cultured at 37°C and the cylinder length was measured with a caliper at various time points over a period of 21 days.

Scaffold mechanical properties of 10 samples per group were tested in uniaxial compression on am Instron 5542 test frame (Norwood, MA). Cylindrical samples measuring approximately 5 mm in length and 8 mm in diameter were cut using a biopsy punch allowed to equilibrate to room temperature and humidity for 24 hours. A pre-load of 1 N was applied to account for non-uniform surfaces and to avoid data capture while samples were not in full contact with compression platens. The upper cross-head was depressed downward at a rate of 0.1% strain/second. The linear elastic modulus, yield stress, and collapse modulus were calculated for both groups. The yield stress was calculated based on the intersection of the linear regression of the linear elastic modulus and the collapse modulus. All data analysis was performed with Bluehill Materials Testing Software Version 2.

Large Animal Model Study Design

Institutional Animal Care and Use Committee approvals were obtained prior to the study. 14 juvenile Yorkshire mini-pigs [age (mean±SD): 3.1±0.2 months; weight: 35±2.2 kg] underwent bio-enhanced ACL repair on the left hind-limb and were randomized into three experimental groups. 6 animals underwent unilateral bio-enhanced ACL repair using ETO scaffolds and 6 animals using EBEAM scaffolds. Additionally, two animals had a bio-enhanced repair with ASEPTIC scaffolds. The right hind-limb was left intact as a control for both groups. The weight bearing status was evaluated by one observer during the mandatory 7-day post-surgical evaluation twice a day qualitatively on a scale from 0–2 (0 = no weight bearing, 1 = touching ground with toe tips, 2 = full weight bearing). Weight of the animals was measured pre-surgery and pre-euthanasia. Knees from two animals each of the ETO and EBEAM group were assessed at 4 and 6 and 8 weeks. Ligament dimensions were recorded using a Vernier caliper, synovium and lymph node tissue were analyzed histologically by two board certified veterinary pathologists at 4, 6, and 8 weeks. At 8 weeks two animals from the ASEPTIC group were analyzed following the same protocol.

Surgical Technique: Bio-enhanced ACL repair

Bio-enhanced ACL repair was performed as previously described.(16) Briefly, a medial arthrotomy and a partial resection of the retropatellar fat pad were performed. The ACL was transected at the junction of the middle and proximal third of its length and a variable depth suture of #1 Vicryl (Ethicon, Somerville, NJ) was placed in the tibial remnant. An Endobutton with three looped #1 Vicryl sutures was threaded through a 4 mm femoral tunnel and flipped to rest on the lateral femoral cortex. Two of the suture loops were passed through the scaffold and a 4 mm tibial drill tunnel and fixed to a button resting on the tibial cortex with the knee in 30° extension. The third suture loop was tied to the suture in the tibial ACL stump. After the scaffold was saturated with 3 ml of autologous blood, the knee was closed in layers.

Following surgery, the animals were housed in individualized pens. After 4, 6, and 8 weeks, two animals randomly selected from each of the ETO and EBEAM groups were euthanized.

At 8 weeks, two animals in the ASEPTIC group were euthanized. Thereafter, knees were opened, ACL dimensions were measured using a caliper and the ACL, synovium and popliteal lymph nodes were harvested for histological assessment.

Qualitative histological assessment of Ligaments, Synovium, and popliteal Lymph Nodes

Qualitative histological assessment was conducted for the anterior cruciate ligaments, synovium, and popliteal lymph nodes for each scaffold group by a board certified veterinary pathologist. Tissues were formalin fixed, embedded in paraffin, sectioned at 5 microns, and stained with hematoxylin and eosin (H&E). Nine sections of each tissue from each animal were evaluated.. Criteria for histopathologic analysis of the ACL were adapted from appendix E of ISO 10993-6 (20) and criteria for synovium from Cake et al. (21) (Table 2). Briefly, the percentage of the ACL slides covered with scaffold material was measured using ImageJ (NIH, Bethesda, MD). Also, the status of the ACL was scored in four different categories – inflammation, neovascularization, fibrosis, and fatty infiltration - synovium in four categories – inflammation, neovascularization, fibrosis, and synovial hypertrophy – and popliteal lymph node in two categories – sinus histiocytosis and follicular hyperplasia.(20, 21) The nine scores per category, tissue and animal were averaged before statistical analysis.

Statistical Analysis

For all assays, the personnel conducting the assay were blinded as to the scaffold group assignations. General linear model was used to model the assay values as a function of treatment group for all outcome measures. Normal distribution of scaffold in vitro assessment data sets was tested using the Kolmogorov-Smirnov test. Data of the scaffold in vitro assessment displayed a normal distribution. Gaussian distribution was assumed for ACL dimensions at 8 weeks (*interval* data with sample size $n=2$). Differences in *in vitro* data and ACL dimensions at 8 weeks between groups were assessed using one-way analysis of variance with Bonferroni correction for multiple comparisons. Differences between the groups in the *ordinal* data of the *in vivo* histological scoring were assessed using Wilcoxon-Mann-Whitney test for time points 4 and 6 weeks (ETO and EBEAM only) and Kruskal Wallis test with Dunn post-hoc test correction for multiple comparisons for the 8 week time point. An alpha value of 5% was considered significant. We report Cohen's d as measure of effect size (calculated as mean difference divided by the pooled standard deviation). An effect size of >0.8 was considered substantial.(22) All data is presented as mean with the 95% confidence intervals. All analyses were performed using intercooled STATA 11 (StataCorpLP, College Station, TX).

RESULTS

Terminal Sterilization

Initial tests showed no microorganism growth-inhibiting property of the scaffolds in the bacteriostasis/fungostasis tests. During the sterility tests 8 out of 8 scaffolds of the ASEPTIC group caused turbidity in the trypticase soy and fluid thioglycollate medium after 7 days consistent with bacterial or fungal growth in this group. However, the scaffold samples of the ETO and EBEAM group did not show any indication of bacterial or fungal growth during incubation in growth medium.

Macroscopic porous structure

Qualitatively, macroscopic porous structure seemed to be homogenous and the pore walls well distinguishable and intact in the ASEPTIC samples (Figure 1A). ETO samples demonstrated partially disrupted porous structure with collapsed pores at some locations (Figure 1B). Macroscopic porous structure of the EBEAM scaffold however seemed to be unchanged by the electron beam sterilization (Figure 1C).

Blood Absorption

The time to soak up 1 ml of whole blood was statistically significantly increased in the ETO scaffold discs compared to ASEPTIC and EBEAM samples (Figure 1D; $P < .001$, $d > 1.26$ for both comparisons)

Protein composition

The protein composition as determined by the SDS-page showed clear and differentiated bands in the ASEPTIC and ETO scaffold group. Most prominent was the typical band pattern for type I collagen with a doublet at apparent molecular weights of 115 and 130 kDa (Figure 2A – yellow arrows). EBEAM samples demonstrated less distinct protein bands with visible subtle background smearing between and below the bands (Figure 2A – red arrows).

Resistance against enzymatic digestion

Treatment with both ETO and EBEAM resulted in a loss of resistance to degradation by collagenase. While the EBEAM samples, on average, had the lowest resistance against collagenase during the first 24 hours, only the one hour time point was significantly lower than that of the ASEPTIC group (Figure 2B, $P < .046$, $d = 0.58$). ASEPTIC scaffolds were still present at 24 hours of exposure to collagenase, while the ETO and EBEAM samples were completely dissolved at 24 hours.

Treatment with EBEAM resulted in a loss of resistance to degradation by elastase. The group treated with EBEAM lost 75% of its length by day 21, while the ASEPTIC and ETO samples had only lost 46% and 50% of their length at the same time point, respectively (Figure 2C). The differences between the ASEPTIC and EBEAM scaffolds were statistically significant at day 2, 7, 14, 21 (Figure 2C, $P < .005$, $d > 0.78$ for all time points). Differences between the EBEAM and ETO samples were also statistically significant at day 1, 14, and 21 (Figure 2C, $P < .025$, $d > 0.91$ for all time points).

Treatment with EBEAM also resulted in a loss of resistance to degradation by plasmin. The EBEAM samples lost 52% of their length over the three weeks, and the ASEPTIC and ETO samples only lost 29% and 35% of their length, respectively. The difference between EBEAM and the ASEPTIC and ETO scaffold samples was statistically significant at day 14, and 21 (Figure 2D, $P < .032$, $d > 0.76$ for all time points).

Scaffold Mechanical Properties

Treatment with EBEAM resulted in a significant increase in average linear elastic modulus and the yield stress compared to the ASEPTIC group, while treatment with ETO

significantly increased the average collapse modulus (Table 3; P = 0.002, P = 0.001, and P = 0.001, respectively).

Animal welfare

All animals recovered well from surgery. Full weight bearing status was achieved within 48–72 hours for all groups. No infection was seen in any of the animals during the 8 week study duration. On average, animals had gained an additional 25.5 ± 2.6 kg in eight weeks. There was no significant difference in weight gain between the groups (P = 1.0).

ACL dimensions

ACL dimensions in the ASEPTIC group were slightly larger than in the ETO or EBEAM group, but no statistically significant difference could be detected (Table 4, P> .2, d< 0.34 for all comparisons)

In-vivo scaffold resorption

At 4 weeks post-surgery, the ACL tissue of the ETO group had a slightly smaller area covered by scaffold material than the EBEAM group, but no statistically significant difference was found despite a substantial effect size (Figure 3A/B, 6% vs. 11% of area on histology slides covered by scaffold, respectively, P= .274, d = 2.1, 4A/B). At 6 weeks there was no scaffold visible on the histology slides of the ETO group and only a few slides showed retained scaffold material on the EBEAM slides (Figure 3A, 0% vs. 0.6%, respectively, P= .794, d = 1.2). At 8 weeks post-surgery all scaffold material was completely resorbed in ASEPTIC, ETO, and EBEAM groups (Figure 3A).

Qualitative histological scoring

ACL - Inflammation

At 4 weeks, the ligament tissue that had been treated with ASEPTIC, ETO and EBEAM scaffolds had minimal lymphohistiocytic inflammation with multifocal aggregates of lymphocytes, histiocytes and fewer plasma cells and broad bands of fibrosis (Figure 4A/B). By 8 weeks, the degree of inflammation was classified as minimal to mild for all groups (Figure 5A). Neither the reduction in inflammation score over time in ETO and EBEAM groups, nor the differences between groups at any time point was statistically significant (Figure 5A, P> .156 and P> .165 for all comparisons, respectively). However, both ETO and EBEAM had a substantial effect when compared with ASEPTIC (d=2.9 and 4.2, respectively)

ACL – Neovascularization

Blood vessels were noted within the scaffold material by the 4 week time point and were present in the ligament wound site through 8 weeks post-surgery in all groups (Figure 4). There was no statistically significant change in any group over time or a statistically significant difference between the groups at any time point (Figure 5B, P> .102 and P> .126 for all comparisons, respectively). However, EBEAM had a substantial effect on the neovascularization compared to ASEPTIC and ETO (d=1.3 and 1.9, respectively)

ACL - Fibrosis

No significant differences were found in the ACL fibrosis score between the treatment groups at any time point (Figure 5C, P> .323 for all comparisons). In all groups at 4 weeks, scaffold material was inter-mixed with regions of fibrous connective tissue. After 6 weeks, fibrosis remained prominent but in some areas there was additional organization of small collagen fibers. At 8 weeks after surgical repair, there were increased areas of organized collagen fibers, but still areas of disorganized collagen as well (Figure 4).

ACL – Fatty infiltration

There was no statistically significant difference in fatty infiltrate of the ACL between groups (Figure 5D, P> .102 for all comparisons). Only ETO showed minimal fatty infiltration at 8 weeks.

Synovium – Inflammation

Over time there was a reduction in synovial inflammation in ETO and EBEAM groups over time, but the reductions were not significantly different (Figure 5E, P> 0.101 for all comparisons). At 8 weeks there was no statistically significant difference in synovial inflammation between ASEPTIC, ETO and EBEAM group (Figure 5E, P> .555 for all comparisons). Effect size at 6 weeks between ETO and EBEAM was substantial (d=1.0).

Synovium – Neovascularization

At all time points, synovial neovascularization was visible but minimal and localized (Figure 6A/C/E). There were no significant differences or substantial effect size in the neovascularization scores between the groups at any time point or between time points within each group (Figure 5F, P> .683 and P> .165 for all comparisons, respectively).

Synovium – Fibrosis

There were no significant differences in the synovial fibrosis scores found between the groups at any time point (Figure 5G, P> .173 and P> .18 for all comparisons, respectively). ASEPTIC compared to the other groups had a substantial effect size (d<2.1 for all comparisons).

Synovium – Hyperplasia

There is no significantly difference between the groups at any time point (Figure 5H, P> . 121 for all comparisons). Synovial hyperplasia scores decreased over time for the ETO and EBEAM group, but not significantly (Figure 5H, P> .156 for all comparisons). However, there was a substantial effect between ETO and EBEAM group (d=1.9).

Popliteal Lymph Node – Sinus Histiocytosis

Mild sinus histiocytosis was seen in the lymph nodes of all treatment groups at all time points (Figure 6B/D/F). Statistically significant difference between ETO and EBEAM group at 4 weeks after surgery (Figure 5I, P< .001, indicated by *, with effect size borderline substantial d<0.7), otherwise there was no difference between groups and time points (Figure 5I, P> .388 and P> .311 for all comparisons, respectively).

Popliteal Lymph Node – Follicular Hyperplasia

Follicular hyperplasia was only detected in the 6 week time point in the EBEAM group (Figures 5J, 6D). The hyperplasia was not seen in the 8 week samples from any group.

DISCUSSION

Treatment of the ECM scaffold using low temperature (>40°C) ethylene oxide for 4.75 hours or electron beam irradiation at 15 kGy resulted in effective sterilization of the scaffold. There were only minor differences in the *in vitro* performance of the treated compared to the aseptic scaffolds for macroscopic pore structure, blood absorption, protein integrity, enzymatic digestion resistance, and scaffold mechanics. The *in vivo* study indicated that ETO treatment of the scaffolds resulted in slightly more blood vessels being present in the wound site and potentially a more rapid resorption of the scaffold material. Equally, histological assessment suggested greater synovial inflammation and hyperplasia, and follicular hyperplasia of the popliteal lymph nodes at 6 weeks in the EBEAM group which resolved by 8 weeks after implantation. However, while some effect sizes were substantial, none of the differences reached statistical significance.

In this current study, ethylene oxide was more destructive to the macroscopic porous structure and hampered the ability of the scaffold to absorb blood to a greater degree than electron beam sterilization. As the key role of the scaffold is to absorb added blood and maintain it in the gap between the torn ligament ends, loss of the absorbent property of the scaffold could be detrimental to its core function and the success of a bridge-enhanced ACL repair. At the same time, ethylene oxide was less detrimental to protein integrity and resistance against enzymatic digestion than electron beam irradiation when evaluated *in vitro*. However, studies show that fibroblast ingrowth into scaffolds over a wide range of pore sizes.(23, 24) And while the prolongation of blood uptake by the ETO treated scaffold was significant, the blood was resorbed eventually and the resorption capacity was not changed. Therefore a localized disintegration of micropores *in vitro* yielding larger overall pore sizes and a prolonged blood absorption time in the ETO scaffolds seems less problematic. A reduced resistance in electron beam irradiated scaffolds against enzymatic degradation *in vitro* could potentially have detrimental effects on outcomes after bio-enhanced ACL repair. Particularly if the scaffold is resorbed *in vivo* by catabolic enzymes in the post-traumatic synovial fluid (18, 19) before it can be replaced by collagenous scar tissue. The biomechanical properties of the dry scaffolds were changed by both terminal sterilization methods. EBEAM increased the stiffness of the scaffold and the ETO treatment decreased compressibility. However, despite the changes in the dry scaffold properties, there was no significant difference in the scaffold resorption rate or histologic response in vivo. This may have been due to the fact that the scaffold is used as a carrier for blood *in vivo* and that the addition of blood may have altered the mechanical properties of the sterilized scaffolds. Thus, the comparison of the ECM-derived scaffolds sterilized by ethylene oxide and electron beam irradiation *in vivo* in an established large animal model for bio-enhanced ACL repair (16, 25–32) was crucial to determine the performance of the sterilized scaffolds and the influence of the changes in *in vitro* scaffold properties have on the healing of the

ACL. The 8 week healing period was chosen based on data finding that this specific scaffold is completely resorbed after eight weeks in vivo.(33).

The *in vitro* results suggest that there are differing negative effects of ethylene oxide and electron beam irradiation on lyophilized ECM-derived scaffolds specifically and thus potentially for sensitive biologic medical devices in general. However, the macroscopic and histologic results after bio-enhanced ACL repair *in vivo* suggest that the sterilization of the ECM-derived scaffolds with either ethylene oxide or electron beam irradiation does not yield a significantly different effect on the *in vivo* outcomes for ligament healing between ETO and EBEAM groups at 4 and 6 weeks after bio-enhanced ACL repair. Similarly, there is no significantly negative effect on the *in vivo* outcome for ligament healing measured at 8 weeks after implantation between the ASEPTIC and the terminal sterilization groups. Further, the size of the healing ACL after 8 weeks was not negatively influenced by the terminal sterilization methods. These *in vivo* results are consistent with a previous study that analyzed the *in vivo* performance of an ethylene oxide sterilized human dermis implant for wound healing after implantation into nude mice, which concluded that graft sterilization with ethylene oxide resulted in good dermal wound healing.(34) Likewise, the study of Rihn et al., who compared ACL reconstruction with bone-patellar tendon-bone autografts or 25 kGy irradiated allograft in human, did not find significant differences between the two groups in age adjusted KT-1000, IKDC knee score, or return to sport.(35) Neither of the mentioned studies utilize a reconstituted form of ECM but rather ECM in its original state, which is due to the lack of studies comparing the effect of terminal sterilization on the *in vivo* performance of reconstituted ECM scaffolds. Still, ethylene oxide and irradiation sterilization also have negative effects on *in vitro* parameters of ECM in its original state. (36) Therefore, changes in *in vitro* properties due to sterilization with ethylene oxide and irradiation might not necessarily influence the *in vivo* performance of either ECM in its original state or, as seen in the current study, reconstituted ECM.

The histological analysis of the repaired ligaments with the terminally sterilized scaffolds in the current study was consistent with earlier studies where the ECM scaffold was almost completely resorbed by 6 weeks.(37, 38) The remaining fibrovascular scar was populated with fibroblasts, vasculature and receding inflammatory tissue reactions were similar to that which occurs in the normal wound healing process.(27, 37–39) Those studies report a gradual repopulation of the wound site with inflammatory cells and fibroblasts, with a peak in cell density at 4 weeks after surgical repair of the ACL.(37, 38) In this study, we used a scaffold that had been decellularized. Prior studies have suggested that the use of non-decellularized tissues, including the RESTORE SIS patch, can lead to an intense inflammatory response in ligament and tendon repair, necessitating removal after implantation in the majority of patients in the clinical trials of such materials (40). Therefore, for this scaffold which could potentially be used clinically in the future, we thought it important to use a decellularized material to minimize the risks of a similar complication. The histological conditions of the ACL repair groups using ethylene oxide and electron beam irradiated scaffolds in the current study at 4, 6, and 8 weeks correspond well with the course of ligament healing observed in these earlier studies.(37, 38)

While EBEAM scaffolds showed a significantly lower resistance against enzymatic degradation than the ETO group *in vitro, in vivo* results suggest that differences in EBEAM and ETO scaffold resorption are mitigated. An explanation for this finding could be the loading of the scaffold with autologous blood before installation *in vivo*. Collagen and fibrin from the blood clot may have formed a matrix that has superior enzymatic resistance than the plain collagen scaffold that was tested *in vitro*.

There are several limitations in this study. The pig model in general has limitations common to all animal models of ACL injury treatment. As a quadruped, the pig's biomechanics slightly differ from the human and, perhaps most importantly, a controlled post-operative rehabilitation plan is difficult to execute. However, the porcine and human knees share multiple anatomic and biomechanical characteristics.(41, 42) In addition, the *in vitro* studies tested the scaffold and only one enzyme at a time, where in the *in vivo* environment, blood and multiple enzymes are present. No fluorescent staining to identify specific ECM molecules was conducted in this study; however, the authors thought that for compositional analysis, the protein blot would be more quantitative and representative of the scaffold as a whole, rather than evaluating a small slice of the scaffold. The power to draw strong conclusions from the qualitatively scored histologic data is limited by the group size of n=2 animals at any time point. However, even given these limitations, the minor differences *in vivo* noted between the ETO and EBEAM group at 4 and 6 weeks and between the ASEPTIC group and the terminal sterilization groups at 8 weeks suggest both, low-temperature ethylene oxide and 15 kGy electron beam irradiation, may be useful for terminal sterilization of lyophilized ECM-derived scaffolds utilized *in vivo*. There was only one sterilization dose tested for electron beam and one combination of processing parameters for ethylene oxide. Certainly, the selection of other doses or processing parameters could have yielded different results in terms of sterility and scaffold function. : No *in vitro* proliferation assays were performed. This was based on findings in previous studies that show that proliferation of cells in vitro on the scaffold material alone is relatively low and limited primarily to the surface of the scaffolds.(43) This is very different to the findings *in vivo*, where the scaffold material is invaded by ovoid, plump fibroblasts no *in vitro* cell proliferation was tested. Therefore the evaluation of *in vivo* cellular infiltration of the scaffolds might be a more relevant assay for this study. This study only addresses bacterial and fungal sterilization and no viruses. However, as previously published (33) we were able to show that the solubilized extracellular matrix derived and lyophilized scaffold was produced free of bovine adventitious viruses. Additionally, the source tissue was meticulously chosen from sources free of bovine encephalopathy to decrease the chance of an animal born viral disease.

In conclusion, the results indicate that minor alterations in the scaffold occur with ethylene oxide and electron beam irradiation, but that these changes do not have a detrimental effect on the clinical and histological outcomes after bio-enhanced ACL repair *in vivo*. Hence, ethylene oxide and electron beam irradiation both appear to be safe and effective techniques for terminal sterilization of ECM-derived scaffolds used in tissue engineering.

ACKNOWLEDGEMENTS

This publication was made possible by Grant Numbers 1RO1-AR056834, 1RO1-AR056834S1 (ARRA), and 2R01-AR054099 from NIAMS/NIH as well as the Lucy Lippit Endowment. Its contents are solely the responsibility of the authors and do not necessarily represent the official views of the NIAMS or NIH. The authors gratefully acknowledge the assistance of many colleagues including Ata Kiapour, Ph.D., Matthew Ackelman, B.A., and Emily Robbins, M.S., for all their help with the animal surgeries, joint harvests, and post-operative testing

REFERENCES

1. 11139:2006. I. Sterilization of health care products - vocabulary. 2006
2. Favero, M. Sterility assurance: concepts for patient safety, in disinfection, sterilization and antisepsis: principles and practices in healthcare facilities, chapter 12. R, WA., editor. Washington: Association for Professionals in Infection Control and Epidemiology. DC.; 2001. p. 110-119.
3. ANSI/AAMI_ST67:2003. Sterilization of health care products - requirements for products labeled “STERILE”. 203.
4. Sun WQ, Xu H, Sandor M, Lombardi J. Process-induced extracellular matrix alterations affect the mechanisms of soft tissue repair and regeneration. Journal of tissue engineering. 2013; 4 2041731413505305.
5. Hemmerich, KJea. Sterilization methods stand the test of time. Medical Device and Diagnostic Industry. 2004; 26(8)
6. 11135-1:2007 AAI. Sterilization of Health Care Products — Ethylene Oxide.
7. 11137:2013 AAI. Sterilization of Health Care Products — Radiation.
8. Standardization IOf. Sterilization of health care products - ethylene oxide - part 1: requirements for development, validation and routine control of a sterilization process for medical devices (ISO 11135-1 :2007). 2007
9. Standardization IOf. Sterilization of health care products - Radiation - Part 2: Establishing the sterilization dose (ISO 11137-2:2012). 2012
10. Chen L, Sloey C, Zhongqi Z, Bondarenko PV, Kim H, Ren D, et al. Chemical Modifications of Therapeutic Proteins Induced by Residual Ethylene Oxide. Journal of pharmaceutical sciences. 2014
11. Freytes DO, Stoner RM, Badylak SF. Uniaxial and biaxial properties of terminally sterilized porcine urinary bladder matrix scaffolds. Journal of biomedical materials research Part, B Applied biomaterials. 2008; 84(2):408–414.
12. Grimes M, Pembroke JT, McGloughlin T. The effect of choice of sterilisation method on the biocompatibility and biodegradability of SIS (small intestinal submucosa). Bio-medical materials and engineering. 2005; 15(1–2):65–71. [PubMed: 15623931]
13. Daly KA, Liu S, Agrawal V, Brown BN, Johnson SA, Medberry CJ, et al. Damage associated molecular patterns within xenogeneic biologic scaffolds and their effects on host remodeling. Biomaterials. 2012; 33(1):91–101. [PubMed: 21967802]
14. Olde Damink LH, Dijkstra PJ, Van Luyn MJ, Van Wachem PB, Nieuwenhuis P, Feijen J. Influence of ethylene oxide gas treatment on the in vitro degradation behavior of dermal sheep collagen. Journal of biomedical materials research. 1995; 29(2):149–155. [PubMed: 7738061]
15. Hoburg A, Keshlaf S, Schmidt T, Smith M, Gohs U, Perka C, et al. Fractionation of high-dose electron beam irradiation of BPTB grafts provides significantly improved viscoelastic and structural properties compared to standard gamma irradiation. Knee Surg Sports Traumatol Arthrosc. 2011; 19(11):1955–1961. [PubMed: 21541710]
16. Murray MM, Fleming BC. Use of a bioactive scaffold to stimulate anterior cruciate ligament healing also minimizes posttraumatic osteoarthritis after surgery. Am J Sports Med. 2013; 41(8): 1762–1770. [PubMed: 23857883]
17. Formulary USPaN. The United States Pharmacopeial Convention: 2010. 2010
18. Kleesiek K, Reinards R, Brackertz D, Neumann S, Lang H, Greiling H. Granulocyte elastase as a new biochemical marker in the diagnosis of chronic joint diseases. Rheumatology international. 1986; 6(4):161–169. [PubMed: 2431451]

19. Kummer JA, Abbink JJ, de Boer JP, Roem D, Nieuwenhuys EJ, Kamp AM, et al. Analysis of intraarticular fibrinolytic pathways in patients with inflammatory and noninflammatory joint diseases. Arthritis Rheum. 1992; 35(8):884–893. [PubMed: 1379429]
20. E AAI-RA. Biological evaluation of medical devices—Part 6: Tests for local effects after implantation. 2010
21. Cake MA, Smith MM, Young AA, Smith SM, Ghosh P, Read RA. Synovial pathology in an ovine model of osteoarthritis: effect of intraarticular hyaluronan (Hyalgan). Clinical and experimental rheumatology. 2008; 26(4):561–567. [PubMed: 18799085]
22. Cohen, J. Statistical Power Analysis for the Behavioral Sciences. 2nd ed. L. Erlbaum Associates; 1988.
23. Salem AK, Stevens R, Pearson RG, Davies MC, Tendler SJ, Roberts CJ, et al. Interactions of 3T3 fibroblasts and endothelial cells with defined pore features. Journal of biomedical materials research. 2002; 61(2):212–217. [PubMed: 12007201]
24. Zeltinger J, Sherwood JK, Graham DA, Mueller R, Griffith LG. Effect of pore size and void fraction on cellular adhesion, proliferation, and matrix deposition. Tissue engineering. 2001; 7(5): 557–572. [PubMed: 11694190]
25. Fleming BC, Magarian EM, Harrison SL, Paller DJ, Murray MM. Collagen scaffold supplementation does not improve the functional properties of the repaired anterior cruciate ligament. J Orthop Res. 2010; 28(5):703–709. [PubMed: 20058276]
26. Fleming BC, Spindler KP, Palmer MP, Magarian EM, Murray MM. Collagen-platelet composites improve the biomechanical properties of healing anterior cruciate ligament grafts in a porcine model. Am J Sports Med. 2009; 37(8):1554–1563. [PubMed: 19336614]
27. Magarian EM, Fleming BC, Harrison SL, Mastrangelo AN, Badger GJ, Murray MM. Delay of 2 or 6 weeks adversely affects the functional outcome of augmented primary repair of the porcine anterior cruciate ligament. Am J Sports Med. 2010; 38(12):2528–2534. [PubMed: 20855556]
28. Murray MM, Magarian EM, Harrison SL, Mastrangelo AN, Zurakowski D, Fleming BC. The effect of skeletal maturity on functional healing of the anterior cruciate ligament. J Bone Joint Surg Am. 2010; 92(11):2039–2049. [PubMed: 20810854]
29. Murray MM, Palmer M, Abreu E, Spindler KP, Zurakowski D, Fleming BC. Platelet-rich plasma alone is not sufficient to enhance suture repair of the ACL in skeletally immature animals: An in vivo study. J Orthop Res. 2009; 27:639–645. [PubMed: 18991345]
30. Murray MM, Spindler KP, Abreu E, Muller JA, Nedder A, Kelly M, et al. Collagen-platelet rich plasma hydrogel enhances primary repair of the porcine anterior cruciate ligament. J Orthop Res. 2007; 25(1):81–91. [PubMed: 17031861]
31. Vavken P, Fleming BC, Mastrangelo AN, Machan JT, Murray MM. Biomechanical outcomes after bioenhanced anterior cruciate ligament repair and anterior cruciate ligament reconstruction are equal in a porcine model. Arthroscopy. 2012
32. Vavken P, Proffen B, Peterson C, Fleming BC, Machan JT, Murray MM. Effects of suture choice on biomechanics and physeal status after bioenhanced anterior cruciate ligament repair in skeletally immature patients: a large-animal study. Arthroscopy. 2013; 29(1):122–132. [PubMed: 23200845]
33. Proffen BL, Perrone GS, Fleming BC, Sieker JT, Kramer J, Hawes ML, et al. Electron beam sterilization does not have a detrimental effect on the ability of extracellular matrix scaffolds to support in vivo ligament healing. J Orthop Res. 2015
34. Chakrabarty KH, Dawson RA, Harris P, Layton C, Babu M, Gould L, et al. Development of autologous human dermal-epidermal composites based on sterilized human allodermis for clinical use. The British journal of dermatology. 1999; 141(5):811–823. [PubMed: 10583161]
35. Rihn JA, Irrgang JJ, Chhabra A, Fu FH, Harner CD. Does irradiation affect the clinical outcome of patellar tendon allograft ACL reconstruction? Knee Surg Sports Traumatol Arthrosc. 2006; 14(9): 885–896. [PubMed: 16502300]
36. Matuska AM, McFetridge PS. The effect of terminal sterilization on structural and biophysical properties of a decellularized collagen-based scaffold; implications for stem cell adhesion. Journal of biomedical materials research Part B, Applied biomaterials. 2015; 103(2):397–406.

37. Joshi S, Mastrangelo A, Magarian E, Fleming BC, Murray MM. Collagen-Platelet Composite enhances biomechanical and histologic healing of the porcine ACL. Am J Sports Med. 2009; 37(12):2401–2410. [PubMed: 19940313]

38. Murray MM, Spindler KP, Ballard P, Welch TP, Zurakowski D, Nanney LB. Enhanced histologic repair in a central wound in the anterior cruciate ligament with a collagen-platelet-rich plasma scaffold. J Orthop Res. 2007; 25(8):1007–1017. [PubMed: 17415785]

39. Mastrangelo AN, Vavken P, Fleming BC, Harrison SL, Murray MM. Reduced platelet concentration does not harm PRP effectiveness for ACL repair in a porcine in vivo model. J Orthop Res. 2011; 29:1002–1007. [PubMed: 21337615]

40. Iannotti JP, Codsi MJ, Kwon YW, Derwin K, Ciccone J, Brems JJ. Porcine small intestine submucosa augmentation of surgical repair of chronic two-tendon rotator cuff tears. A randomized, controlled trial. J Bone Joint Surg Am. 2006; 88(6):1238–1244. [PubMed: 16757756]

41. Proffen BL, McElfresh M, Fleming BC, Murray MM. A comparative anatomical study of the human knee and six animal species. The Knee. 2012; 19(4):493–499. [PubMed: 21852139]

42. Xerogeanes JW, Fox RJ, Takeda Y, Kim HS, Ishibashi Y, Carlin GJ, et al. A functional comparison of animal anterior cruciate ligament models to the human anterior cruciate ligament. Annals of biomedical engineering. 1998; 26(3):345–352. [PubMed: 9570217]

43. Murray MM, Martin SD, Spector M. Migration of cells from human anterior cruciate ligament explants into collagen-glycosaminoglycan scaffolds. J Orthop Res. 2000; 18(4):557–564. [PubMed: 11052491]

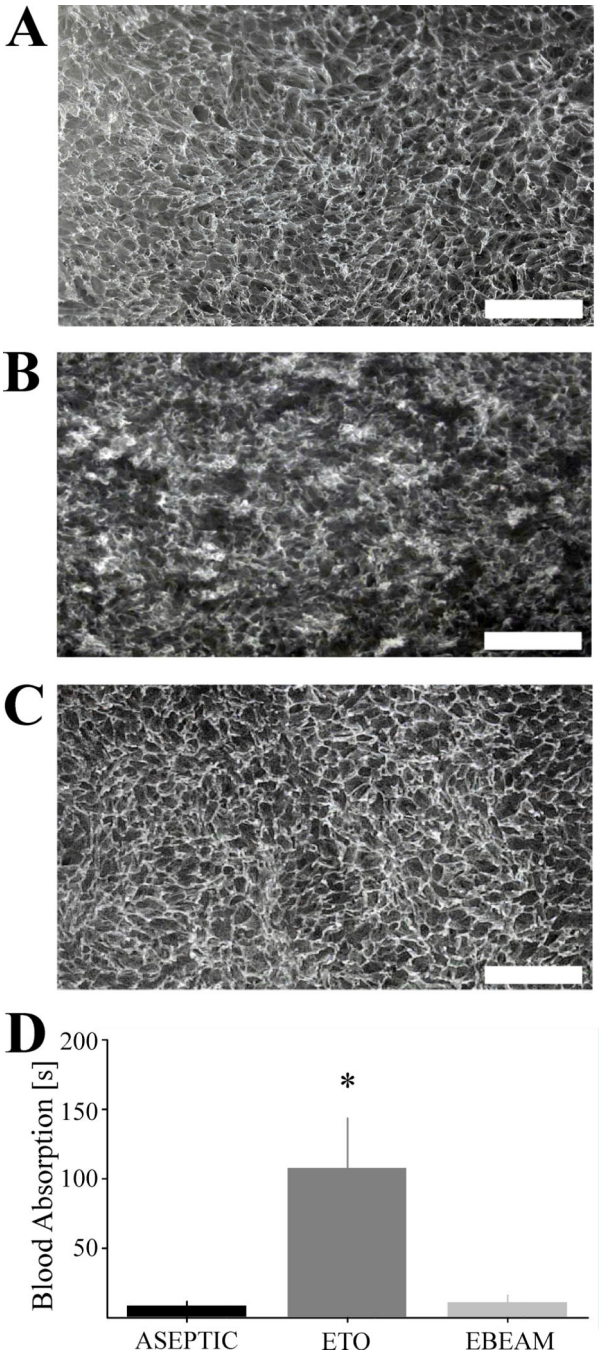

Figure 1. Macroscopic scaffold pore structure and blood absorption time

A – Scaffold pore structure of representative ASEPTIC sample is homogenous and the pore walls well distinguishable and intact (white bar = 1 mm); **B** - Scaffold pore structure of representative ETO sample shows partially disrupted porous structure with collapsed pores (white bar = 1 mm); **C** - Scaffold pore structure of representative EBEAM sample is similar to the ASEPTIC group (white bar = 1 mm); **D** – Blood absorption time of ETO group significantly prolonged compared to ASEPTIC and EBEAM group (*, P< .001, *d* >1.26 for both comparisons)

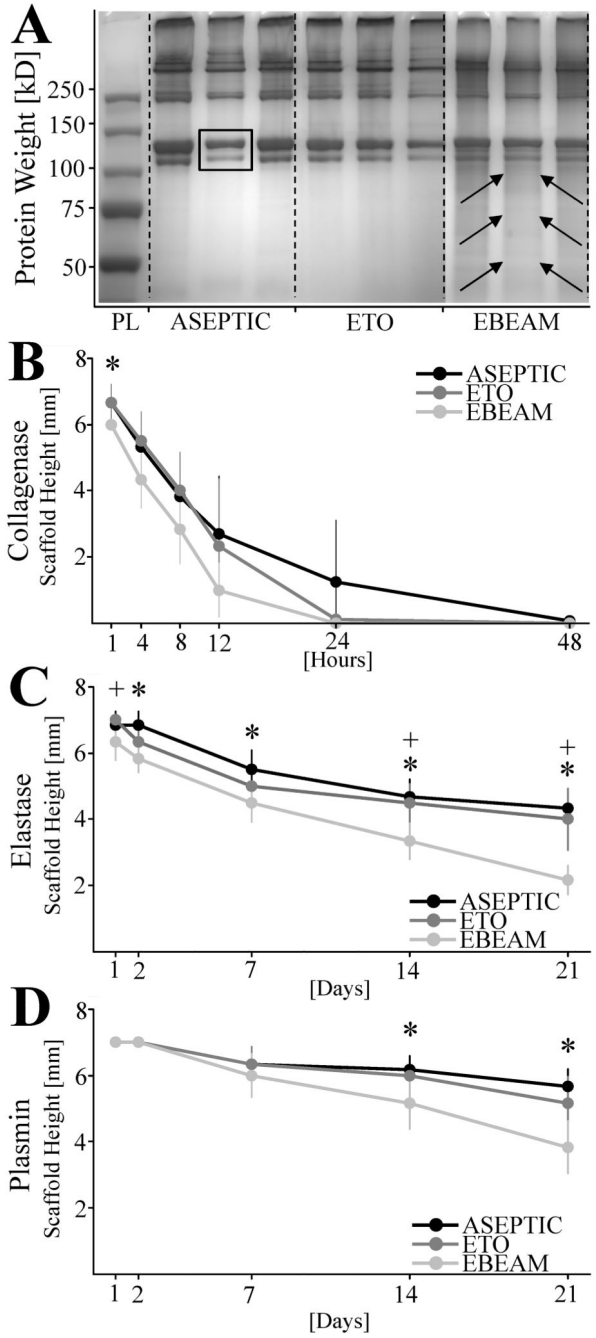

Figure 2. SDS-PAGE and resistance against collagenase, elastase, and plasmin digestion of ASEPTIC, ETO, and EBEAM scaffolds

A - Distinct protein bands in all ECM scaffold groups with typical band pattern for type I collagen with a doublet at apparent molecular weights of 115 and 130 kDa (yellow arrows). EBEAM samples demonstrated less distinct protein bands with visible subtle background smearing between and below the bands (red arrows). **B** – Length of scaffold samples during digestion with collagenase [mm]. EBEAM scaffolds digest significantly quicker than ASEPTIC and ETO samples at day 1 (*, P≤ .046, *d* = 0.58). **C** - Length of scaffold samples

during digestion with elastase [mm]. EBEAM scaffold samples are significantly more digested than ASEPTIC samples at day 2, 7, 14, 21 (* $P \leq .005$, $d > 0.91$ for all time points) and ETO samples at day 1, 14, and 21 ($^{+}$, $P \leq .025$ for all time points). **D** - Length of scaffold samples during digestion with plasmin [mm]. EBEAM scaffolds digest significantly quicker than ASEPTIC and ETO samples at day 14 and 21 (*, $P \leq .032$, $d > 0.76$ for all time points).
PL – Protein ladder
kD – Kilo Dalton
SDS-PAGE – Polyacrylamide gel electrophoresis

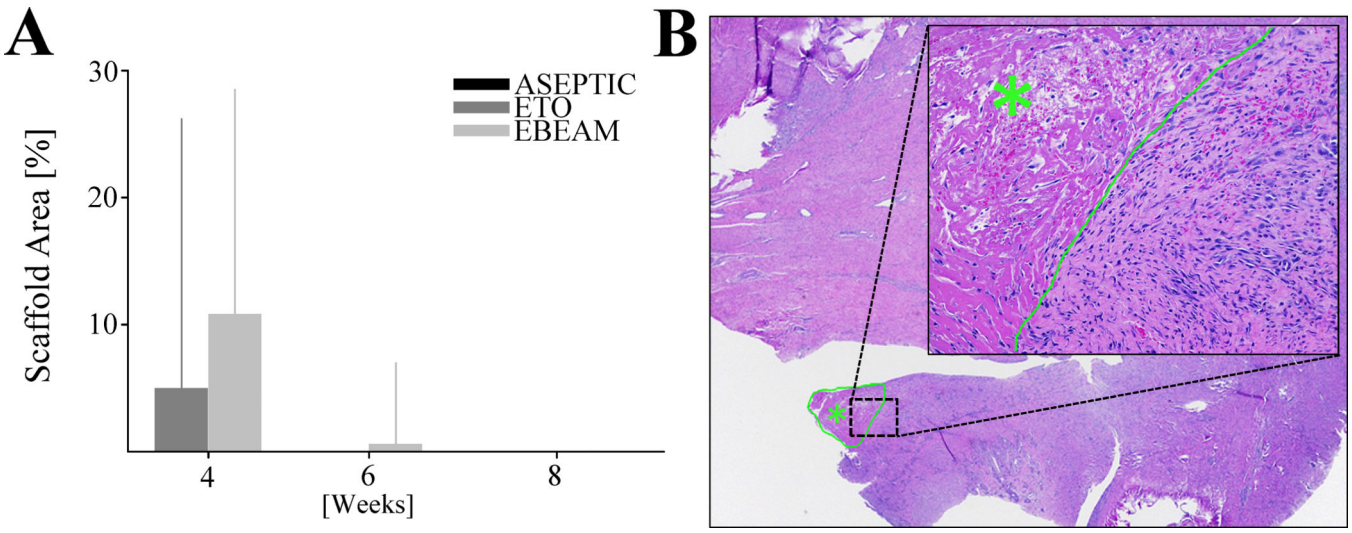

Figure 3. Scaffold resorption

A - Percentage of ACL sections covered by scaffold material at 4, 6, and 8 weeks. No statistically significant difference between EBEAM and ETO after 4/6 weeks. At 8 weeks there were no scaffold residuals left in any group. Aseptic group was only tested at 8 weeks and did not show any scaffold residuals. **B** - H&E stained ACL section from EBEAM group after 6 weeks (20× magnification) with scaffold residual (green outline/star). Inset showing scaffold area (200× magnification), border between scaffold area (green star) and adjacent connective tissue green. Scaffold material characterized as acellular eosinophilic material. The scaffold material was not associated with significant inflammation or hemorrhage but did have some fibrous ingrowth.

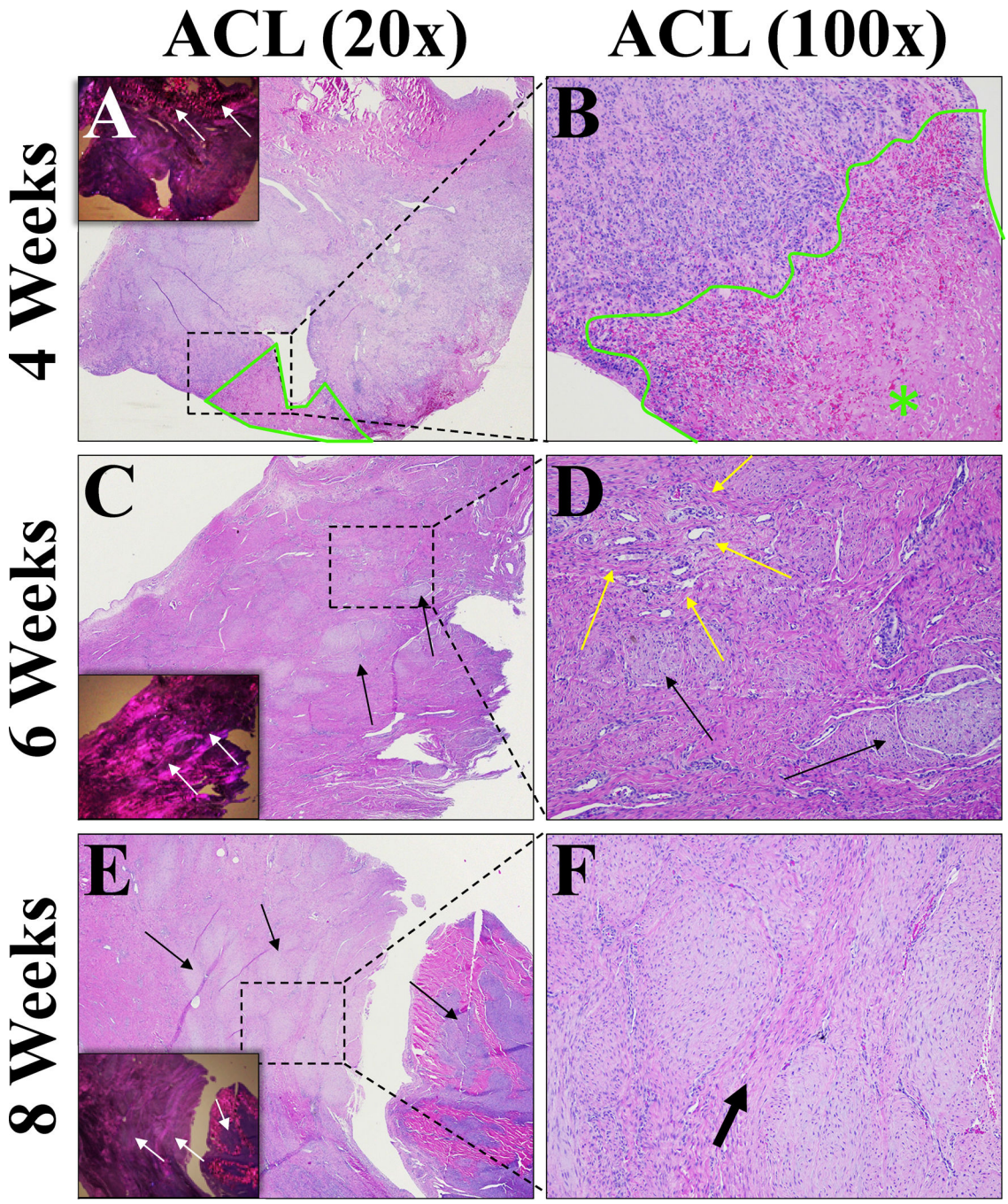

Figure 4. Histological ACL sections representative of all treatment groups

A – H&E stained ACL section after 4 weeks (20× magnification). Inset showing section under polarized light to visualize collagen crimp. Prominent fibrosis, mature collagen is birefringent (top of inset – white arrows) while fibrosis is not. Small amount of scaffold residual outlined and marked with green star. **B** - 100× magnification of dashed rectangular area of picture (A) to visualize cells. Small amount of scaffold material on bottom right (scaffold area outlined and marked with green star) associated with moderate lymphohistiocytic inflammation (predominantly macrophages and lymphocytes admixed

with fibrous connective tissue and fibroblasts). **C** - H&E stained ACL section after 6 weeks (20× magnification). Inset showing section under polarized light to visualize collagen crimp. Slight reduction in fibrosis compared to 4 weeks, but still prominent. Fibrosis visible under polarized light as dark areas (inset – white arrows) which correspond to the more lightly stained areas in standard HE sections (black arrows). **D** - 100× magnification of dashed rectangular area in picture (E) to visualize cells. Neovascularization visible (yellow arrows) as well as fibrosis (black arrows) which separates normal collagen bundles. **E** - H&E stained ACL section after 8 weeks (20× magnification) Inset showing section under polarized light to visualize collagen crimp. Fibrosis prominent, visible as lightly stained areas on HE sections (black arrows) and darker areas under polarized light (white arrows). In this section, the area at right stained darker and fibrosis is bluer in color. **F** - 100× magnification of dashed rectangular area in picture (E) to visualize cells. Organized fibrosis is clearly visible separating bands of normal collagen (thick arrow). Scattered inflammatory cells, but inflammation is minimal to mild overall.

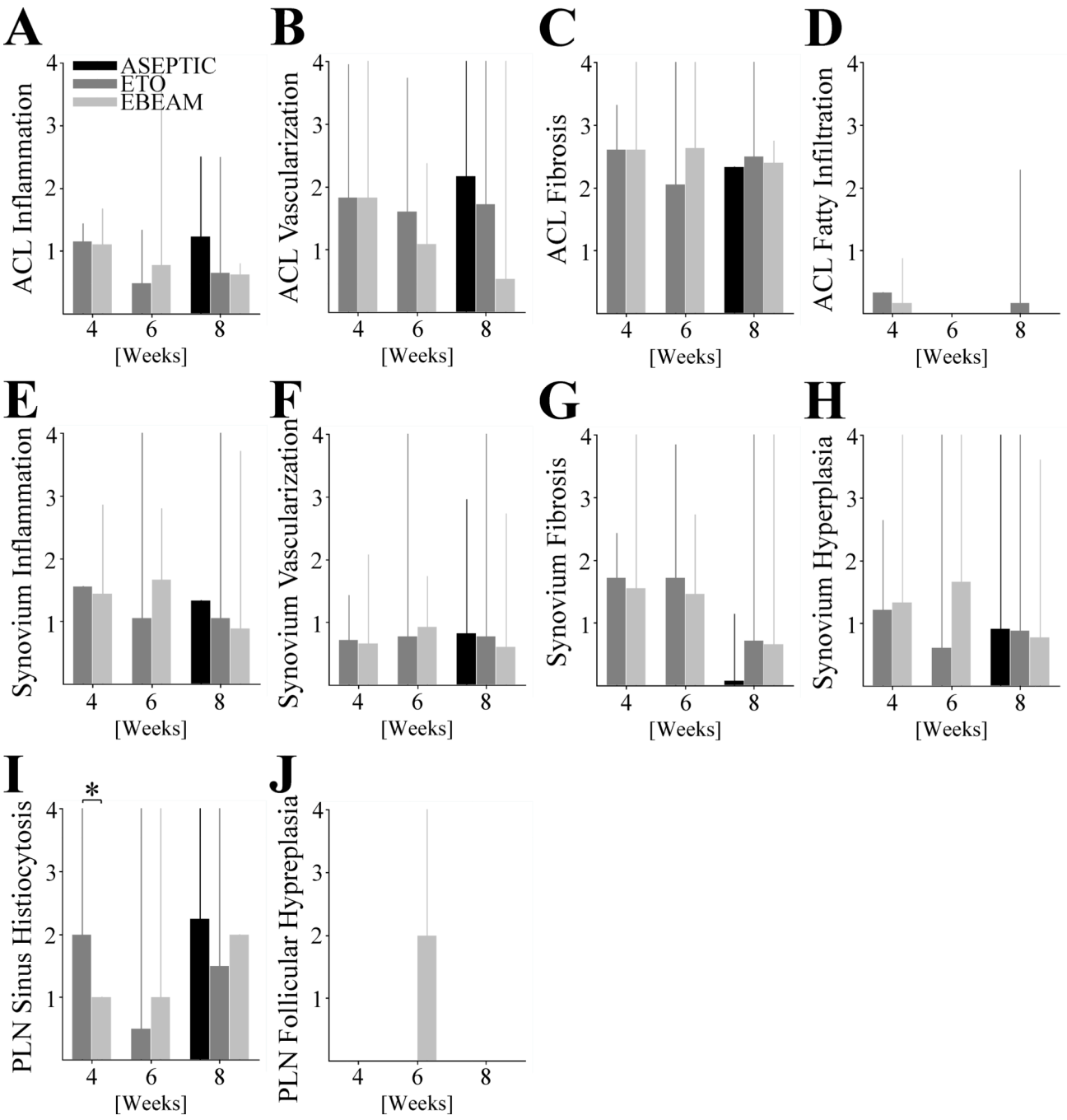

Figure 5. Histological Scoring of Anterior Cruciate Ligament (ACL), Synovium, and Popliteal Lymph Node (PLN)

Barplots indicating mean and spikes 95% CI of **A** - ACL inflammation, **B** – ACL neovascularization, **C** - ACL fibrosis, and **D** - ACL fatty infiltration, as well as **E** - synovial inflammation, **F** - synovial neovascularization, **G** - synovial fibrosis, and **H** - synovial hypertrophy, and also **I** - popliteal lymph node sinus histiocytosis (* indicating statistical significant difference with P< .001 and large effect size of $d = 1.41$) and **J** - popliteal lymph

node follicular hyperplasia at 4, 6, and 8 weeks for ETO and EBEAM and at 8 weeks for ASEPTIC group.

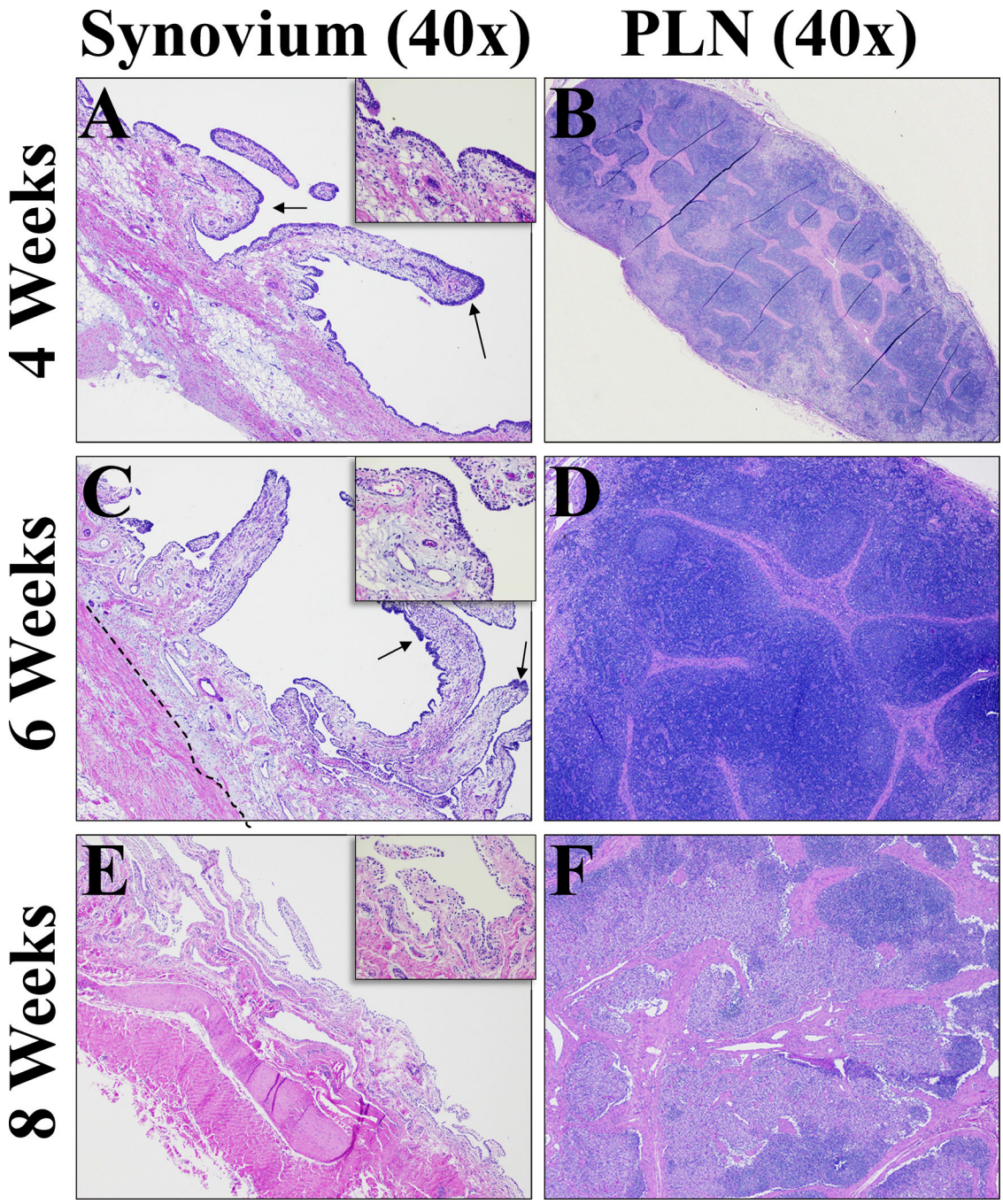

Figure 6. Histological sections from synovium and popliteal lymph node (PLN) representative of all treatment groups

A - H&E stained synovium section after 4 weeks (40× magnification). Diffusely thickened intima, multifocal areas of prominent hyperplasia (arrows). Subintimal inflammation present consistent with ongoing healing. Fibrosis slightly increased. **B** - H&E stained popliteal lymph node section after 4 weeks (40× magnification). Prominent sinus histiocytosis consistent with mild lymphadenopathy as a result of draining inflammation from implant site, not considered an adverse reaction. **C** - H&E stained synovium section after 6 weeks

(40× magnification).Still multifocal areas of hyperplasia (arrows), but overall intima thin and lined by 1–2 cells as seen in control tissues. Subintimal fibrosis remained increased (dashed line). **D** - H&E stained popliteal lymph node after 6 weeks (40× magnification). Mild follicular and paracortical and sinus histiocytosis. **E** - H&E stained synovium section after 8 weeks (40× magnification). Resolution of intimal hyperplasia, subintimal fibrosis and inflammation. Collagen fibers approach thin intimal layer.**F** - H&E stained popliteal lymph node section at 8 weeks after bio-enhanced ACL repair 40× magnification for a general view. Follicular and paracortical and sinus histiocytosis continues to resolve.

Table 1

Study design

Scaffold Group	n	Sterility Testing	Porous Structure and Blood Absorption	SDS-PAGE and Enzymatic Resistance	Scaffold Mechanical Testing	In Vivo 4 Weeks	In Vivo 6 Weeks	In Vivo 8 Weeks
ASEPTIC	26	8	3	3	10			2
ETO	30	8	3	3	10	2	2	2
EBEAM	30	8	3	3	10	2	2	2

n = Initial scaffold number per group
ASEPTIC = non-terminally sterilized ECM-derived scaffolds
ETO = Ethylene oxide sterilized ECM-derived scaffolds
EBEAM = Electron beam irradiation sterilized ECM-derived scaffolds
SDS-PAGE = Sodium dodecyl sulfate polyacrylamide gel electrophoresis

Table 2

Criteria used to score the anterior cruciate ligament, synovium, and popliteal lymph node

ANTERIOR CRUCIATE LIGAMENT		SYNOVIUM		POPLITEAL LYMPH NODE	
CRITERIA	**pts**	**CRITERIA**	**pts**	**CRITERIA**	**pts**
INFLAMMATION (Macrophages, polymorphonuclear, plasma, giant cells)		**INFLAMMATION (Macrophages, polymorphonuclear, plasma, giant cells)**		**SINUS HISTIOCYTOSIS**	
				None	0
				Minimal	1
None observed	0	None	0	Mild	2
Rare, 1–5/40× field	1	Minimal – Scattered small aggregates	1	Moderate	3
5–10/40× field	2	Mild – More numerous small aggregates or diffuse infiltration by small numbers of cells	2	Severe	4
Heavy Infiltrate	3				
Packed	4			**FOLLICULAR HYPERPLASIA**	
		Moderate – Numerous large aggregates or diffuse infiltration by a large number of cells	3	None	0
NEOVASCULARIZATION				Minimal	1
None	0			Mild	2
Minimal capillary proliferation, focal, 1–3 buds	1	Marked – Diffuse infiltration by large numbers of cells	4	Moderate	3
				Severe	4
Groups of 4–7 capillaries with supporting fibroelastic structures	2	**NEOVASCULARIZATION**			
Broad band of capillaries with supporting structures	3	0–10 vascular formations/60× field	0		
		11–15 vascular formations/60× field	1		
Extensive band of capillaries with fibroelastic structures	4	16–20 vascular formations/60× field	2		
		21–25 vascular formations/60× field	3		
		26–30 vascular formations/60× field	4		
FIBROSIS					
None	0	**FIBROSIS**			
Narrow band	1	None	0		
Moderately thick band	2	Minimal subintimal fibrosis – loose wavy fibers separated by edema	1		
Thick band	3				
Extensive band	4	Mild subintimal fibrosis – thicker and more organized fibers extending slightly further from the synoviocyte lining layer	2		

ANTERIOR CRUCIATE LIGAMENT		SYNOVIUM		POPLITEAL LYMPH NODE	
CRITERIA	**pts**	**CRITERIA**	**pts**	**CRITERIA**	**pts**
FATTY INFILTRATE					
None	0	Moderate subintimal fibrosis – thick bands of fibrosis extending subintimally	3		
Minimal amount of fat associated with fibrosis	1	Marked subintimal fibrosis – diffuse marked fibrosis	4		
Several layers of fat and fibrosis	2				
Elongated and broad accumulation of fat cells at the implant site	3	**SYNOVIAL HYPERPLASIA**			
Extensive fat completely surrounding the implant	4	Normal synoviocyte lining layer, 1–2 cell layers thick	0		
		Minimal hyperplasia – Focal areas of synoviocyte hyperplasia that are 3–4 cell layers thick	1		
		Mild hyperplasia – Diffusely 3–4 cell layers thick +/− focal areas up to 5 cell layers thick	2		
		Moderate hyperplasia – Diffusely 5–7 cell layers thick +/− focal areas up to 10 layers thick	3		
		Marked hyperplasia - Diffusely 8+ cell layers thick	4		

pts - points

J Biomater Appl. Author manuscript; available in PMC 2016 October 01.

Table 3

Linear Elastic Modulus (LEM), Yield Stress, and Collapse Modulus (CM) of ASEPTIC and EBEAM scaffolds, n = 10.

	Scaffold Group	LEM [kPa]	95% CI	Yield Stress [kPa]	95% CI	CM [kPa]	95% CI
Absolute Values	**ASEPTIC**	701	808 593	67.8	76.3 59.3	173	188 158
	ETO	706	908 506	67.2	77.3 57.1	103	116 92
	EBEAM	1270	1613 927	106	124.4 87	147	172.3 121.9
Comparison P-Values	**ASEPTIC vs. ETO**	1.0		1.0		0.001	
	ASEPTIC vs. EBEAM	0.002		0.001		0.095	
	ETO vs. EBEAM	0.002		0.001		0.002	

95% CI – 95% confidence interval
LEM – Linear Elastic Modulus
CM – Collapse Modulus

Table 4

Comparison of ACL dimensions at two months after surgery at harvest between aseptic, ETO, and EBEAM treatment groups. n = 2. No comparisons are considered significant or substantial with P-values >0.2 and *d*-values <0.34.

Surgical Group	ACL Length	95% CI	ACL Width	95% CI	ACL Depth	95% CI	ACL Volume	95% CI
ASEPTIC	34.0	69.6 −1.6	5.5	7.3 3.7	11.1	58.1 −35.9	2515	22453 −17451
ETO	29.3	38.8 19.7	5.8	27.4 −15.7	12.7	30.5 −5.1	2209	10899 −6480
EBEAM	32.6	54.8 10.3	5.9	23.0 −11.3	10.6	24.4 −7.3	2017	3479 554
P-value	>0.2		>0.55		1.0		1	
***d*-value**	<0.34		<0.04		<0.28		<0.05	

95% CI – 95% confidence interval
ACL – Anterior cruciate ligament